Fast Energy Migration in Pyronine-Loaded Zeolite L Microcrystals

Niklaus Gfeller, Silke Megelski, and Gion Calzaferri*

Department of Chemistry and Biochemistry, University of Bern, Freiestrasse 3, CH-3000 Bern 9, Switzerland

Received: October 13, 1998

The stacking of pyronine and oxonine in the channels of zeolite L microcrystals is possibly due to their high affinity for entering the channels and to the narrowness of inside the channels, which prevents the dyes from gliding past each other. This allowed us to invent experiments for observing energy migration in pyronine-loaded zeolite L microcrystals of cylinder morphology. Organic dyes have the tendency to form aggregates at relatively low concentrations which cause fast thermal relaxation of electronic excitation energy. The role of the zeolite is to prevent this aggregation even at very high concentrations and to superimpose a specific organization. Light is absorbed by a pyronine molecule located somewhere in one of the zeolite channels. The excitation energy migrates preferentially in both directions along the axis of the cylinder because of the pronounced anisotropy of the system. It is eventually trapped by an oxonine located at the front or at the back of the microcrystal. This process is called front−back trapping. The electronically excited oxonine then emits the excitation with a quantum yield of approximately one. The pronounced anisotropy of the electronic transition moments of both pyronine and oxonine can be observed in an optical fluorescence microscope by means of a polarizer. Maximum luminescence appears parallel to the longitudinal axis of the cylindrical microcrystals, extinction appears perpendicular to it, and their base always appears dark. We report experimental results for the front−back trapping efficiency of pyronine-loaded zeolite L microcrystals of different average lengths, namely 700, 1100, and 1500 nm, different pyronine occupation probability, ranging from 0.03 to 0.48; and modification at the base with oxonine as luminescent traps. Extremely fast electronic excitation energy migration along the axis of cylindrical crystals has been observed, supported by the increase of the effective excitation lifetime caused by self-absorption and re-emission of the pyronine vertical to the cylinder axis. Effective energy migration lengths of up to 166 nm upon pyronine excitation have been observed, which thus leads to the remarkable properties of this material.

1. Introduction

Zeolite microcrystals can act as hosts for the supramolecular organization of molecules, complexes, and clusters, thus encouraging the design of precise functionalities.[1−9] The main role of the zeolite framework is to provide the desired geometrical properties for arranging and stabilizing the incorporated species. Focusing on supramolecularly organized dye molecules in the channels of hexagonal zeolite L crystals, we have shown that they provide fascinating possibilities for building an artificial *antenna device* which consists of highly concentrated monomeric dye molecules of up to 0.4 M with a large Förster energy transfer radius and a high luminescence quantum yield in a specific geometrical arrangement.[5,7−9] Organic dye molecules have the tendency to form aggregates at much lower concentrations, and such aggregates are known to cause fast thermal relaxation of electronic excitation energy. The role of the zeolite is to prevent this aggregation and to superimpose a specific organization, which is possible as we have shown recently.[9] In such an antenna, light is absorbed by one of the strongly luminescent chromophores. Because of short distances and the alignment of the electronic transition dipole moments of the dyes along the channels, the excitation energy is transported by preferentially Förster-type energy migration along the axis of the cylindrical antenna to a specific trap. The ideal dimension of a microcrystal containing several million chromophores is

* Corresponding author. Tel: +41 31 631 4226. E-mail: calza@solar.iac.unibe.ch
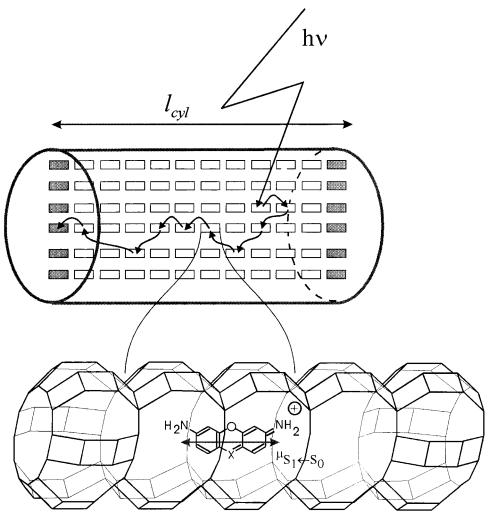
less than a micrometer. A completely different approach for constructing nanometer-sized species with light-harvesting properties has been followed by Balzani and co-workers[10] and has led to beautiful dendrimeric transition metal compounds.

We recently demonstrated that the intercalation of pyronine and oxonine molecules into the linear channels of zeolite L can be visualized with a fluorescence microscope.[9] One can observe the alignment of the dyes in the channels by means of a polarizer, because maximum luminescence appears parallel to the longitudinal axis of the microcrystals, and extinction appears perpendicular to it. Furthermore the cylindrical microcrystals always appear dark at their base. A simple experiment for the visual proof of the energy transfer from pyronine to oxonine in zeolite L is based on the observation that both dyes are intercalated from an aqueous solution within about the same time leading to short donor−acceptor distances, which allow efficient energy transfer between them. The formation of aggregates, which can act as unwanted traps, is prohibited for spatial reasons. Hence, there are no such traps inside the microcrystals. The dyes are arranged with their long molecular axes along the linear channels, and they cannot glide past each other because the linear channels are too narrow. This allows the filling of specific parts of the microcrystals with a desired type of dye.

Theoretical considerations of energy migration as a series of Förster energy transfer steps have shown that energy migration rate constants of up to 30 steps/ps can be expected in a material of this kind.[8] This is faster than in the antenna system of natural

Pyronine-Loaded Zeolite L Microcrystals

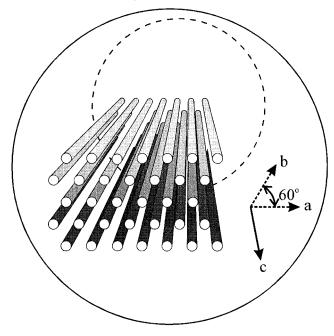*J. Phys. Chem. B, Vol. 103, No. 8, 1999* **1251**

SCHEME 1:   Schematic Representation of a Cylindrical Microcrystal Consisting of Supramolecularly Organized Pyronine Molecules (X = CH), Indicated by Empty Rectangles, and an Oxonine (X = N) Trap at the Front and the Back of Each Channel, Indicated by Shaded Rectangles. The Enlargement Shows a Detail of the Zeolite L Channel with a Dye Molecule and Its Electronic Transition Moment, Which Is Aligned along the Channel Axis.

photosynthetic organisms, where approximately 0.2 steps/ps have been reported.[11,12] In this first report on experimentally observed energy migration along the axis of pyronine-loaded cylindrical zeolite L microcrystals, we show that it is possible to realize at least part of these theoretical predictions. The principle of the system investigated is illustrated in Scheme 1, where the empty bars represent pyronine molecules located in the channels of zeolite L, and the dashed bars are oxonine molecules that act as luminescent traps at both ends of the cylinder. We define the occupation probability p as the ratio between the number of sites occupied by a dye and the total number of sites available. Hence, p adopts values between 0 for an unloaded zeolite and 1 for a zeolite loaded to its maximum. The enlargement shows a zeolite L channel with a pyronine molecule (X = C−H), the electronic transition moment $\mu_{S_1 \leftarrow S_0}$ of which is aligned along the channel axis. A schematic view illustrating the parallel-lying channels filled with pyronine monomers is given in Scheme 2. The primitive vector **c** corresponds to the channel axis, whereas the primitive vectors **a** and **b** are perpendicular to it, enclosing an angle of 60°.[13,14] A feeling for the material is obtained by realizing, for instance, that a zeolite L microcrystal of 700 nm length and a diameter of 600 nm gives rise to about 95 000 parallel-lying channels, each of which bears a maximum of 470 sites for the pyronine

molecules. So far up to two thirds of the 1.5-nm-long sites available in zeolite L have been filled by us with chromophores.

In the experiments reported, light is absorbed by a pyronine molecule located somewhere in one of the channels. The excitation energy can then migrate along the axis of the microcrystal, as indicated by the arrows in Scheme 1, and is eventually trapped by an oxonine located at the front or at the back of the cylinder. The electronically excited oxonine then emits the excitation with a quantum yield of approximately one. This process, which we call front−back trapping, has been investigated theoretically for energy migration occurring by Förster[15] energy transfer. We found that a total front trapping efficiency of up 99.8% can be obtained for microcrystals of 50 nm length, if all sites are occupied by a pyronine chromophore.[8] Self-absorption and re-emission were not considered in this theoretical study, which focused on crystals of about 50 nm. However, for crystals with larger dimensions, particularly larger diameter, pyronine-pyronine self-absorption and re-emission are expected to contribute significantly to the energy migration properties. We now describe experiments investigating the front−back trapping efficiency independently of the mechanism that governs the energy migration. They are based on the fact that pyronine-loaded zeolite L microcrystals, modified with one oxonine molecule at the front and at the back of each channel

SCHEME 2:   Schematic View of Some Channels in a Hexagonal Zeolite. The Dimension of the Channels and the Dyes Have to Be Chosen So That the Dyes Can Enter as Monomers Only. a, b, and c represent the Lattice Constants of the Hexagonal Framework.

on average, can be prepared as illustrated in Scheme 1 and that it is possible to synthesize zeolite L microcrystal cylinders of different average lengths with narrow size distribution. Microcrystals with an average length of 700, 1100, and 1500 nm have been investigated.

2. Experimental Section

2.1. Physical Measurements. UV/vis absorption spectra were recorded with use of a Perkin-Elmer Lambda 14 spectrophotometer. For the absorption measurements of aqueous zeolite L suspensions (6.7×10^{-4} g zeolite L per milliliter, which corresponds to approximately 10^9 zeolite microcrystals per milliliter), the spectrophotometer was equipped with an integrating sphere (Labsphere RSA-PE−20). For the fluorescence measurements the suspensions contained about 3×10^{-5} g zeolite L per milliliter. Emission spectra were carried out on a Perkin-Elmer LS 50B spectrofluorimeter. In both cases 10-mm-path length quartz cuvettes were used. The crystallinity and the morphology of the zeolite L samples were investigated by X-ray powder diffraction and scanning electron microscopy, respectively.

2.2. Materials. Zeolite L with the stoichiometry $K_9(SiO_2)_{27}$-$(AlO_2)_9 \cdot 21H_2O$ (M = 2883 g/mol) was synthesized using silica (AEROSIL-Dispersion, K330; Degussa), Al(OH)$_3$ (Fluka, purum), and KOH (Fluka, Biochemical). Pyronine and oxonine with perchlorate as counterion were synthesized and purified according to the procedure in the literature.[7,16,17] The extinction coefficients of pyronine ($\epsilon_{max} = 8.3 \times 10^4$ L mol^{-1}cm^{-1}) and of oxonine ($\epsilon_{max} = 7.8 \times 10^4$ L mol^{-1}cm^{-1}) reported by Müller[16] and Bonneau and Joussot-Dubien,[18] respectively, were used in all subsequent measurements to determine the concentration of the corresponding dye solutions.

2.3 Synthesis of Zeolite L. Al(OH)$_3$ was dissolved at 100 °C in a solution consisting of KOH and water and then under vigorous stirring added to a mixture of colloidal silica and water. After a few minutes this mixture, which had turned into a thick

gel, was transferred into a pressure tight PTFE reaction vessel. Crystallization followed without stirring at 160 °C within 6 days. After cooling, the upper part of the strongly alkaline solution was decanted. The white residue was washed with hot water until it remained neutral. It was then air-dried for 14 h at 100 °C and stored at room temperature in a closed flask. Cylindrical microcrystals of different lengths were obtained by varying the K_2O/Al_2O_3 ratio and the water content. An initial solution with the molar ratio of 3.0 K_2O, 1.0 Al_2O_3, 10.7 SiO_2, 169.3 H_2O leads to zeolite L microcrystals of 700 nm in length and 600 nm in diameter, on average. With an initial solution with a molar ratio of 3.0 K_2O, 1.0 Al_2O_3, 10.7 SiO_2, 182.0 H_2O we obtained zeolite L microcrystals with a length of 1100 nm and a diameter of 700 nm, whereas a stoichiometry of 2.6 K_2O, 1.0 Al_2O_3, 9.7 SiO_2, 161.3 H_2O yields microcrystals with a length of 1500 nm and a diameter of 950 nm, on average. This procedure differs in some details with respect to the synthesis of zeolite L reported in the literature.[19]

2.4. Preparation and Characteristics of Dye-Loaded Zeolite L. The dye-loaded zeolite L microcrystals, used for the investigations of energy migration, were prepared as follows: 100 μL zeolite L suspension (1 g/50 mL) was added to 3 mL doubly distilled water containing 800 μL of a 1.04×10^{-4} M aqueous pyronine solution. This suspension was treated in an ultrasonic bath for 10 min in order to avoid aggregation of the microcrystals and was refluxed overnight. This yields a pyronine loading (occupation probability p_{py}) of 0.24, where p is defined as

$$p = \frac{\text{number of dye molecules}}{\text{number of sites}} \quad (1)$$

Under these conditions an equal distribution of pyronine in the microcrystals is obtained. The equilibrium constant K for the exchange reaction is defined as follows:[20]

$$D_S^+ + K_Z^+ \rightleftharpoons D_Z^+ + K_Z^+ \quad (2)$$

where D_S^+ is the dye in the solution, D_S^+ is the dye in the zeolite, K_Z^+ is the cation in the zeolite, and K_S^+ is the cation in the solution,

$$K = \frac{[D_Z^+][K_S^+]}{[D_S^+][K_Z^+]} \quad (3)$$

The equilibrium constants for pyronine and oxonine in a potassium zeolite L were $>10^3$ at room temperature (RT). The spectral overlap of the absorption and fluorescence spectra of pyronine at RT was determined as $J_{pypy} = 1.05 \times 10^{-13}$ cm^3 M^{-1} and the spectral overlap for the pyronine-emission and oxonine-absorption as $J_{pyox} = 1.29 \times 10^{-13}$ cm^3 M^{-1}.[8]

2.5. Modification of Pyronine-Loaded Zeolite L Microcrystals with Oxonine Traps for Front−Back Trapping Experiments. Because of the large equilibrium constant of pyronine and oxonine ($K > 10^3$) and because the dye molecules cannot glide past each other in the narrow channels, it is possible to modify a pyronine-loaded zeolite with oxonine in a precise way, see section 3.1. According to eq 3 in ref 8 the total number (n) of sites per channel is:

$$n = \frac{l_{cyl}}{u \cdot |c|} \quad (4)$$

where $|c|$ is the length of the primitive vector c and u is the number unit cells per site. For pyronine and oxonine in zeolite

Pyronine-Loaded Zeolite L Microcrystals

J. Phys. Chem. B, Vol. 103, No. 8, 1999 **1253**

L, where $|c|$ is 0.75 nm, any site spans two unit cells. For oxonine to occupy two sites per channel, the following occupation probability p_{ox} is required:

$$p_{ox} = \frac{2}{n} = \frac{2 \cdot u \cdot |c|}{l_{cyl}} \tag{5}$$

On average one oxonine molecule is added to both ends of each channel. To do this for the 700-nm material, for example, 50 μL oxonine solution of 2.9×10^{-5} M was added to the total volume of a suspension prepared as described in section 2.4 and boiled under reflux for 0.5 h. This yields an oxonine occupation probability p_{ox} of 0.0042.

2.6. Measurements of Energy Migration. Pyronine and oxonine were much more stable in "self-synthesized" zeolite L then in the commercial product from Union Carbide, which was used in previous work.[7,21] The reason for this is not clear, but it must be related to reactive sites (impurities) present in the commercial material. To measure the energy migration the samples were excited at 470 nm where only pyronine absorbs light, and the fluorescence spectra of pyronine and oxonine were monitored. After specific excitation of pyronine, the electronic excitation either causes pyronine fluorescence or migrates along the pyronine molecules until it reaches an oxonine trap, where it causes oxonine fluorescence.

3. Results and Discussion

The trapping function $T(t)$ is defined as the probability that the electronic excitation reaches a trap during the time period t after irradiation. The trapping efficiency T_∞ is equal to the sum of the excitation probabilities of all trapping sites at infinite time after irradiation. In a system where donors and traps have a luminescence quantum yield of one and where the traps are excited exclusively by receiving energy from the donors, the trapping efficiency corresponds to the ratio of the luminescence intensity of the traps I_T divided by the total luminescence I_{tot}:

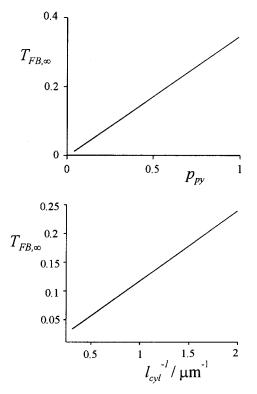$$T_\infty = \frac{I_T}{I_{tot}} \tag{6}$$

It is sufficient that the donor and the acceptor molecules have equal fluorescence quantum yields for eq 6 to hold. We have discussed in a previous report that it is convenient to distinguish between different types of trapping, which we named according to the position of the traps.[8] In this context we focus on front–back trapping $T_{FB}(t)$, which refers to traps on the front and on the back of a cylindrical microcrystal. Front–back trapping is governed by energy migration along the channel axis. In the experiments described here, the donors that absorb light are pyronine whereas the traps are oxonine molecules and their luminescence intensity is I_{py} and I_{ox}, respectively. We will show that the system described fulfills the conditions needed for the front–back trapping efficiency $T_{FB,\infty}$ to be given by:

$$T_{FB,\infty} = \frac{I_{ox}}{I_{py} + I_{ox}} \tag{7}$$

The migration length l_{mig} corresponds to the mean distance an electronic excitation can travel during the natural lifetime τ_{py}. It is related to the average rate constant for energy migration from a site i to a site j, $\langle k_{ij} \rangle$ by[15,22]

$$l_{mig} = \sqrt{a \langle k_{ij} \rangle \tau_{py}} \tag{8}$$

where a is a constant. We have shown that the energy migration

Figure 1. Front–back trapping efficiency $T_{FB,\infty}$ as a function of the occupation probability p_{py} for microcrystals of about 700 nm (above) and as a function of the inverse length of the cylindrical microcrystals $(l_{cyl})^{-1}$ for an occupation probability p_{py} of 0.5 (below).

rate constant k_{ij} in this system is proportional to the square of the occupation probability of the pyronine p_{py}^2 multiplied by the spectral overlap J_{pypy}.[8]

$$k_{ij} \propto p_{py}^2 J_{pypy} \tag{9}$$

From this it follows that l_{mig} fulfills the following proportionality:
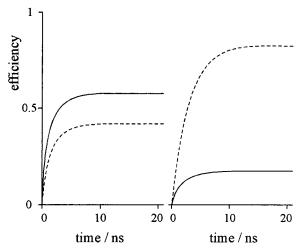
$$l_{mig} \propto p_{py} \sqrt{J_{pypy}} \tag{10}$$

The total luminescence intensity $I_{py} + I_{ox}$ is determined by the length of the microcrystal l_{cyl}. The excitation energy migrating in both directions can be trapped, hence, the oxonine luminescence intensity I_{ox} is given by twice the migration length l_{mig}. The front–back trapping efficiency $T_{FB,\infty}$ can therefore be expressed as:

$$T_{FB,\infty} = \frac{2 l_{mig}}{l_{cyl}} \tag{11}$$

From this and eq 7 it is possible to determine the migration length experimentally as a function of the pyronine occupation probability by monitoring the front–back trapping at different p_{py} and/or l_{cyl} independent of the mechanism:

$$l_{mig} = \frac{l_{cyl}}{2} \cdot \frac{I_{ox}}{I_{py} + I_{ox}} \tag{12}$$

The theoretically determined $T_{FB,\infty}$, as a function of the occupation probability p_{py} for a microcrystal of 700 nm and as a function of the length of the cylindrical microcrystals l_{cyl} for a given p_{py} of 0.5, is reported in Figure 1. It is proportional to the occupation probability and also to the inverse length of the
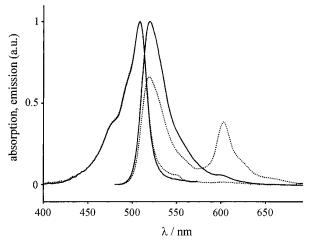
Figure 2. Competition between front−back trapping $T_{FB}(t)$ (solid) and pyronine fluorescence $F(t)$ (dashed) of a pyronine-loaded zeolite L cylinder of 200 nm (left) and of 700 nm (right) length and diameter with $p = 0.5$, for parallel orientation of the chromophores and thus parallel orientation of all electronic transition dipole moments with respect to the cylinder axis.

Figure 3. Absorption and fluorescence spectra of pyronine-loaded zeolite L microcrystals of 700-nm average length and a loading p_{py} of 0.24 (solid). Absorption and fluorescence spectra of the same microcrystals after they have been modified with one oxonine at both sides of each channel (dotted). The excitation wavelength for the fluorescence spectra was 470 nm.

cylinders, as stated in eqs 10 and 11, respectively. The calculations have been carried out the same way as those reported in Figure 10 of ref 8. This means that self-absorption and re-emission have not been included and that the results characterize a reference system with only energy migration, trapping, and luminescence. Deviations from the theoretical finding can therefore be used for identifying additional processes that might occur in the microcrystals. The results illustrated in Figure 1 indicate that two kinds of measurements should lead to relevant information for characterizing the energy migration of the pyronine-loaded zeolite microcrystals. The first is to measure the front−back trapping efficiency $T_{FB,\infty}$ as a function of the occupation probability p_{py} and the second is to measure $T_{FB,\infty}$ as a function of the length of the microcrystals l_{cyl}. In the following sections we describe experiments that allowed us to monitor quantitatively energy migration in pyronine-loaded zeolite L microcrystals by using oxonine as a luminescent trap.

3.1. Detecting Energy Migration by Trapping with a Luminescent Dye. The principle of this experiment is as follows: First, the microcrystals are ion exchanged with pyronine up to the desired loading p_{py}. Second, a calculated amount of oxonine is added to the suspension such that one oxonine molecule enters on both sides of each channel on average. This is the simplest way to realize experimentally the situation illustrated in Scheme 1. It works because of the much larger affinity of these dyes for the inside of the channels than for the outer surface, as long as there is sufficient free channel space available. The competition between front−back trapping $T_{FB}(t)$ and pyronine fluorescence $F(t)$ in a pyronine-loaded zeolite L cylinder can be calculated as described in ref 8. The results so obtained are reported in Figure 2. They show that the front−back trapping can compete well in microcrystals of 200 nm length, but that it becomes inefficient for microcrystals of 700 nm. We will see below that this changes significantly by taking into account the anisotropic pyronine self-absorption and re-emission occurring in our system.
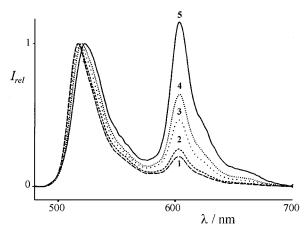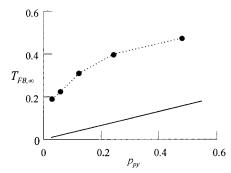
Before proceeding we report an observation that makes the interpretation of the experimental results especially easy. The fluorescence quantum yields of pyronine and oxonine in water at room temperature were found to be approximately 1, and their decay times were 2.3 ns and 3.2 ns, respectively.[7] These characteristics remained about the same after intercalating the

dyes into zeolite L. Figure 3 illustrates that the decrease in pyronine luminescence is compensated quantitatively by the increase of oxonine luminescence, when the oxonine is used as a front−back trap for pyronine-loaded microcrystals. The solid lines in this figure correspond to the absorption and fluorescence spectra of the 700-nm pyronine-loaded zeolite L with a loading p_{py} of 0.24. The dashed curves correspond to the absorption and fluorescence spectra after the microcrystals have been modified on both ends with one monolayer of oxonine traps ($p_{ox} = 0.0042$). We observed that the absorption spectrum is affected only slightly by the oxonine modification in the 600-nm region, whereas the pyronine luminescence is significantly reduced by the oxonine traps but fully compensated by the oxonine luminescence. It is sufficient to compare the peak heights because of the similarity of the shape of the pyronine and the oxonine fluorescence spectra. Integrating the bands leads to the same result. This proves that the pyronine and the oxonine quantum yields are indeed the same under these conditions and that it is correct to use eq 7 for analyzing the data. It also proves that emission of the oxonine comes only from oxonine excited by pyronine−oxonine energy transfer because the so-called trivial energy transfer caused by pyronine emission and oxonine reabsorption is negligible because of the low oxonine loading ($p_{ox} = 0.0042$). This conclusion is supported by the results reported in ref 9 where a simple and elegant experiment for the visual proof of the efficient energy transfer from pyronine to oxonine in zeolite L is described. We would also like to remember that the absorption and emission of both, pyronine and oxonine in zeolite L, are highly anisotropic and occur only *perpendicular to the cylinder axis* (which coincides with the channel axis). This can easily be observed with the help of a fluorescent microscope.

3.2. Energy Migration as a Function of the Occupation Probability. The front−back trapping efficiency $T_{FB,\infty}$ can be used to determine the migration length l_{mig}, which in turn serves to estimate the length of a microcrystal at which light harvesting within its volume and transport to its front and back surfaces remains efficient. From this it is easy to derive the characteristics of front trapping alone.[8] We therefore have measured the fluorescence spectra of the oxonine-modified, pyronine-loaded zeolite, as a function of the pyronine loading p_{py} for microcrystals of about 700 nm. Results of these measurements are

Pyronine-Loaded Zeolite L Microcrystals

J. Phys. Chem. B, Vol. 103, No. 8, 1999 **1255**

Figure 4. Energy migration in pyronine-loaded microcrystals as observed by the oxonine fluorescence at different pyronine loadings p_{py}. **1**, $p_{py} = 0.03$; **2**, $p_{py} = 0.06$; **3**, $p_{py} = 0.12$; **4**, $p_{py} = 0.24$; **5**, $p_{py} = 0.48$. We show the relative intensity I_{rel} of fluorescence spectra recorded after specific excitation of only pyronine molecules at 470 nm scaled to the same height at the maximum of the pyronine emission. The amount of front−back-located oxonine traps corresponds to one molecule at the front and one at the back of each channel in all samples.
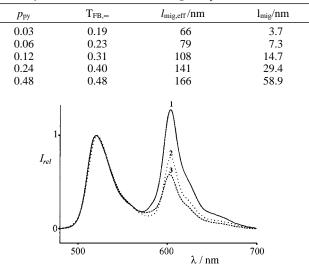

Figure 5. Energy migration in pyronine-loaded microcrystals. The front−back trapping efficiency $T_{FB,\infty}$ is shown as a function of different pyronin loadings p_{py}. The experimental data (dots) correspond to those in Figure 4. The calculated data (solid) have been obtained by neglecting self-absorption and re-emission.
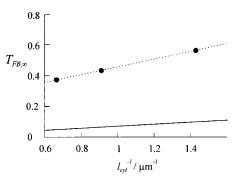
reported in Figure 4. The excitation wavelength was 470 nm, and the spectra were normalized to equal height at the pyronine emission maximum. The spectra illustrate the increase of the oxonine emission with its maximum at 605 nm. Although the maximum of the pyronine emission shifts from 515 to 522 nm with increasing loading p_{py}, we observed that the maximum of the oxonine emission remains at the same position. The shift of the maximum in the pyronine is caused by self-absorption, which becomes more and more important with increasing pyronine concentration. Because the oxonine concentration is always the same and always very low, the emission maximum does not shift. From the data shown in Figure 4 we derive the front−back trapping efficiency $T_{FB,\infty}$ as a function of p_{py} according to eqs 10 and 11. This is shown in Figure 5 where we compare it with the theoretical value. The theoretical values have been calculated in the same way as those illustrated in Figure 1, by neglecting self-absorption and re-emission. It is obvious that the observed trapping efficiency $T_{FB,\infty}$ is much larger than the calculated values. We also observe that $T_{FB,\infty}$ levels off at large p_{py}. From this we determine the effective migration length $l_{mig,eff}$ by using eq 12. The values reported in Table 1 show that the effective migration length is already astonishingly large for a low pyronine loading.

3.3. Energy Migration in Microcrystals of Different Lengths. It would be interesting to compare the calculated

TABLE 1: Experimentally Observed Front−Back Trapping Efficiency $T_{FB,\infty}$, Effective Migration Length $l_{mig,eff}$, and Migration Length l_{mig}, Calculated for Förster-Type Energy Migration, as a Function of the Pyronine Loading p_{py} for Microcrystals of About 700 nm Length ($l_{cyl} = 700$ nm)

p_{py}	$T_{FB,\infty}$	$l_{mig,eff}$/nm	l_{mig}/nm
0.03	0.19	66	3.7
0.06	0.23	79	7.3
0.12	0.31	108	14.7
0.24	0.40	141	29.4
0.48	0.48	166	58.9

Figure 6. Energy migration in pyronine-loaded microcrystals as observed by the oxonine fluorescence at constant pyronine loading of $p_{py} = 0.36$ but for microcrystals of different length l_{cyl} modified with one oxonine trap at the front and one at the back of each channel. **1**, $l_{cyl} = 700$ nm; **2**, $l_{cyl} = 1100$ nm; **3**, $l_{cyl} = 1500$ nm. l_{cyl} corresponds to the average length of the microcrystals. We show the relative intensity I_{rel} of the fluorescence spectra recorded after specific excitation of only pyronine at 470 nm. The spectra have been normalized to equal height at the pyronine emission maximum at 515 nm.
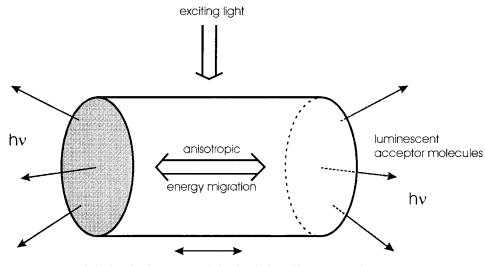

Figure 7. The front−back trapping efficiency $T_{FB,\infty}$ is shown as a function of the inverse length of the microcrystal $l_{cyl}-1$. The experimental data (dots) correspond to those shown in Figure 6. The calculated data (solid) have been obtained by neglecting self-absorption and re-emission.

dependence of the front−back trapping efficiency, $T_{FB,\infty}$, as a function of the length of the cylindrical microcrystals l_{cyl} and for a given occupation probability, p_{py}, with experimental results. Microcrystals of different lengths must be available, for this reason we have been able to prepare such material, which has a narrow distribution of the cylinder length. The procedure is described in the Experimental Section. This allowed us to study energy migration on pyronine-loaded zeolite L with average lengths of 700, 1100, and 1500 nm, modified with oxonine traps on both ends. The morphology of the microcrystals used in these experiments is the same as reported in Figure 2 of ref 9.

The experimental results reported in Figures 6 and 7 have been obtained for microcrystals with $l_{cyl} = 700$, 1100, and 1500 nm. All samples had the same pyronine loading, $p_{py} = 0.36$, and were modified with the same amount of front−back-located oxonine traps corresponding to one molecule at the front and one at the back of each channel. The excitation wavelength was

SCHEME 3: Illustration of the Anisotropic Properties of a Dye-Loaded Zeolite L Microcrystal.

470 nm, and the spectra where normalized to equal height at the pyronine emission maximum at 515 nm. The spectra illustrate nicely the decrease of the oxonine trap emission with its maximum at 605 nm with increasing average length of the cylinders. We note that the maximum of the pyronine emission as well as the maximum of the oxonine emission remain at the same position in the three samples because the local dye concentration is the same in each case. Again, interpretation of the results is straightforward. The longer the cylinder, the longer it takes an excitation to reach the oxonine trap at the front or at the back of the microcrystal. This means that the probability for an electronic excitation to be trapped by an oxonine decreases with the increasing length of the microcrystals. To compare these results with the theoretical results illustrated in Figure 1, in Figure 7 we report the observed trapping efficiency $T_{FB,\infty}$ as a function of the inverse length of the microcrystals l_{cyl}. It is obvious that the trapping efficiency is much better than what was calculated.

3.4. Self-absorption and Re-emission. Self-absorption and re-emission are well known to give rise to a systematic lengthening of measured fluorescence lifetimes.[23] Different geometries have been investigated for this process by Hammond.[24] Although pyronine−oxonine reabsorption and re-emission processes can be neglected in all experiments we have described, it was not surprising to find that pyronine−pyronine self-absorption and re-emission play an important role in the material discussed in this article. We also expect that total internal reflection cannot be neglected despite the fact that the dimension of the microcrystals is similar to the wavelength of the light with which we are working. We cannot yet give a full quantitative account of these processes in the material investigated. However, a simple estimate of where self-absorption and re-emission come in is useful to obtain an idea of the order of magnitude at which they play a role. The concentration, even in the material with the lowest occupation probability of $p_{py} = 0.03$, corresponds to a 1.2×10^{-3} M solution, whereas it corresponds to a 0.2 M solution for $p_{py} = 0.48$. One must realize further that the pronounced anisotropic ordering of the electronic transition moments along the axis of the cylinder causes a molar extinction coefficient three times larger than the one measured in a solution in which the transition moments are randomly distributed in space. The simplest geometrical situation we can imagine is an infinitely extended anisotropic and very thick layer containing a certain concentration of dyes lying parallel to the

yz-surface and all oriented in the same direction which we chose to be *z*. Light of low intensity comes in perpendicularly (*x*-direction) to the *yz*-surface. Part of it is reflected and the major part enters the layer, depending on the difference of refractive indices. The light penetrating the sample is absorbed according to Beer's law and its intensity decays accordingly. A molecule that has been excited can either perform energy transfer to one of its neighbors or it can emit a photon in the $\pm x$ and $\pm y$ direction. Only photons emitted in $-x$ direction have a chance to leave the layer, according to Beer's law, and depending on the refractive index of the material and the environment, they can also be back-reflected. To get a rough idea we consider a spectral range in which the molar extinction coefficient for the incident photon is the same as for the re-emitted photon. Neglecting the cosine-square dependence of the transition probability, one finds that 50% of the photons re-emitted in $-x$ direction are reabsorbed. This means that a maximum of 1/8 of the incident photons reach the surface from the inside in the $-x$ direction, where they can either leave the material or be reflected.

Coming back to the microcrystals, it is obvious that the effective energy migration length $l_{mig,eff}$ is affected by these processes. Because front−back trapping is governed by processes perpendicular to the absorption and re-emission, we assume that eq 8 is still valid and that we can substitute the natural lifetime of the pyronine molecules τ_{py} by an effective lifetime τ_{eff} of the excitation inside of a microcrystal. Time-resolved measurements and measurements at different temperatures carried out by us do support this interpretation.

3.5 Conclusions. We have shown that zeolite L microcrystals can act as hosts for supramolecular organization of strongly luminescent organic dyes in their one-dimensional channels. Extremely fast electronic excitation energy migration along the axis of cylindrical crystals has been demonstrated in pyronine-loaded zeolite L modified with oxonine as luminescent traps. We have good evidence that the antenna properties of this system are governed by Förster-type energy migration, supported by an increase of the effective excitation lifetime because of self-absorption and re-emission. However, more detailed photochemical and photophysical studies of this fascinating system are needed to fully understand the processes that take place. Many other highly organized dye-zeolite materials of this type can be prepared and are expected to show a wide variety of remarkable properties.[5] Characteristics of the material investi-

Pyronine-Loaded Zeolite L Microcrystals

J. Phys. Chem. B, Vol. 103, No. 8, 1999 **1257**

gated are explained in Scheme 3, which emphasizes on the pronounced anisotropy for light absorption/emission and energy migration. They provide different possibilities for building sophisticated artificial antenna devices. In addition, the largely improved chemical and photochemical stability of dye molecules intercalated in an appropriate zeolite framework allows us to work with dyes that otherwise would be considered uninteresting because of lack of stability.[5] New electronic structures are accessible by specific geometrical arrangements. The structure of the host and the techniques for arranging zeolite microcrystals of good quality and narrow size distribution as dense monograin layers on different substrates can be used to realize specific properties.[25,26]

References and Notes

(1) Ramamurthy, V. *Photochemistry in Organized and Constrained Media*; VCH Publishers: New York, 1991. Ramamurthy, V. *Chimia* **1992**, *46*, 359.

(2) Schüth, F. *Chem. Uns. Zeit* **1995**, *29*, 42.

(3) Lainé, P.; Lanz, M.; Calzaferri, G. *Inorg. Chem.* **1996**, *35*, 3514. Calzaferri, G.; Lanz, M.; Li, J. W. *J. Chem. Soc., Chem. Commun.* **1995**, 1313.

(4) Brühwiler, D.; Gfeller, N.; Calzaferri, G. *J. Phys. Chem B* **1998**, *102*, 2923.

(5) Calzaferri, G. *Chimia* **1998**, *52*, 525.

(6) Werner, L.; Caro, J.; Finger, G.; Kornatowski, J. *Zeolites* **1992,** *12*, 658. Ehrl, M.; Deeg, F. W.; Bräuchle, C.; Franke, O.; Sobbi, A.; Schulz-Ekloff, G.; Wöhrle, D. *J. Phys. Chem.* **1994**, *98*, 47. Caro, J.; Marlow, F.; Wübbenhorst, M. *Adv. Mater.* **1994,** *6*, 413. Wöhrle, D.; Schulz-Ekloff, G. *Adv. Mater.* **1994**, *6*, 875. Hoffmann, K.; Marlow, F.; Caro, J. *Zeolites* **1996**, *16*, 281.

(7) Binder, F.; Calzaferri, G.; Gfeller, N. *Sol. Energy Mater. Sol. Cells* **1995**, *38*, 175. Binder, F.; Calzaferri, G.; Gfeller, N. *Proc. Indian Acad. Sci (Chem. Sci.)* **1995**, *107*, 753.

(8) Gfeller, N.; Calzaferri, G. *J. Phys. Chem. B* **1997**, *101*, 1396.

(9) Gfeller, N.; Megelski, S.; Calzaferri, G. *J. Phys. Chem B* **1998**, *102*, 2433.

(10) Balzani, V.; Campagna, S.; Denti, G.; Juris, A.; Seroni, S.; Venturi, M. *Acc. Chem. Res.* **1998**, *31*, 26.

(11) Kühlbrandt, W.; Wang, D. N. *Nature* **1991**, *350*, 130. Fetisova, Z. G.; Freiberg, A. M.; Timpmann, K. E. *Nature* **1988**, *334*, 633.

(12) Hu, X.; Schulten, K. *Phys. Today* **1997**, 28.

(13) Meier, W. M.; Olson, D. H.; Baerlocher, Ch. *Atlas of Zeolite Structure Types*; Elsevier: London, 1996.

(14) Ohsuna, T.; Horikawa, Y.; Hiraga, K. *Chem. Mater.* **1998**, *10*, 688.

(15) Förster, T. *Ann. Phys. (Leipzig)* **1948**, *2*, 55. Förster, T. *Fluoreszenz organischer Verbindungen;* Vandenhoeck & Ruprecht; Göttingen, 1951.

(16) 1Müller, W. *Liebigs Ann. Chem.* **1974**, 334.

(17) Fiedeldei, U. Ph.D. Thesis, Freie Universität Berlin, Germany, 1988.

(18) Vogelmann, E. Ph.D. Thesis, Universität Stuttgart, Germany, 1974. Bonneau, R.; Joussot-Dubien, J. *Z. Phys. Chem., Neue Folge* **1976**, *101*, 225.

(19) Ernst, S.; Weitkamp, J. *Catal. Today* **1994**, *19*, 27. Tsapatsis, M.; Okubo, T.; Lovallo, M.; Davis, M. E. *Mater. Res. Soc. Symp. Proc.* **1995**, *371*, 21.

(20) Breck, D. W. *Zeolite Molecular Sieves*; John Wiley & Sons: New York, 1974.

(21) Calzaferri, G.; Gfeller, N. *J. Phys. Chem.* **1992**, *96*, 3428.

(22) Einstein, A. *Ann. Phys.* **1906**, *19*, 371.

(23) Baumann, J.; Calzaferri, G.; Hugentober, T. *Chem. Phys. Lett.* **1985**, *116*, 66.

(24) Hammond, P. R. *J. Chem. Phys.* **1979**, *70*, 3884. Hammond, P. R.; Nelson, R. *IEEE J. Quantum Electron.* **1980**, *QE−16*, 1161.

(25) Lainé, P.; Seifert, R.; Giovanoli, R.; Calzaferri, G. *New J. Chem.* **1997**, *21*, 453.

(26) Scandella, L.; Binder, G.; Gobrecht, J.; Jansen, J. C. *Adv. Mater.* **1996**, *8*, 137.